Nanotechnology for microbiology

The term “microbiology” generally describes the study of those organisms invisible to the human eye, in particular yeast, bacteria and viruses. However, these three types of organisms are significantly different from each other. Yeast and bacteria are different cell types (eukaryotic and prokaryotic respectively), whereas a virus is not strictly a living organism, being an obligate intracellular parasite. The tools to conduct research in microbiology can be separated into two main fields- microscopy, which is required for visualization, and molecular biology, which has been used to characterize (in some cases comprehensively) the genetic and proteomic make up of these organisms.

The initial steps in opening the field of microbiology came with the advent of the first microscopes. Bacteria were first visualized by Antony van Leeuwenhoek, using a simple, self-built microscope, around 1676. The microscopes built by Leeuwenhoek were not compound microscopes, relying instead on a single lense, more like a very powerful magnifying glass. One of his first descriptions of bacteria (referred to as animalcules) was from samples scraped from the teeth of van Leeuwenhoek himself.

While yeast have been used in fermentation and to leaven bread for around 5000 years, it was in 1860 that Louis Pasteur first described the yeast, Saccharomyces cerevisiae as the effecter of these processes. Louis Pasteur made many significant contributions to the field of microbiology over the years, from the description of S. cerevisiae, to his elegant experiments to disprove the theory of spontaneous generation and his fundamental role in the germ theory of disease and early vaccine development. In fact, one of Pasteur’s successes in the field of vaccine development was to attenuate rabies virus through heating for injection as a vaccine, despite not being able to visualize the virus itself in the affected tissue.

Advancements made in light microscopy by the combined work of Ernst Abbe and Carl Zeiss in the 1880s further extended the research of the microbiological world. However, as Abbe himself described, there is a limit to the resolution of light microscopy, dependent on the wavelength of the illuminating light and the numerical aperture of the lens. In reality, the resolution of light microscopy is limited to half the wavelength of light, or around 250 nm. As such, the study of the structure of viruses had to wait for the advent of the electron microscope in 1931 by Ernst Ruska and the subsequent crystallization of the tobacco mosaic virus in 1935 by Wendall Stanley.

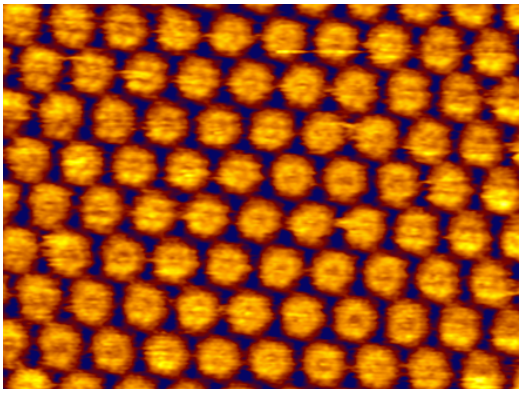

Fig. 1 HPI layer from Deinococcus radiodurans, image kindly provided by Dr. Patrick Frederix, University of Basel.

More recently, the atomic force microscope has opened a new path for the investigation and manipulation of structures on a very small scale. One of the most often cited advantages of the AFM in the study of biological structures is the fact that, unlike electron microscopy, high resolution images can be obtained under physiological conditions. However, there is more to the AFM than just its capacity for high resolution imaging. The mechanical nature of the AFM means that the cantilever, used for imaging, can also be used to measure interaction forces, in the piconewton range.

As such, not only can the AFM image the surface of microorganisms at high resolution, under physiological conditions, it can also be used to investigate the binding forces between microorganisms and target surfaces.

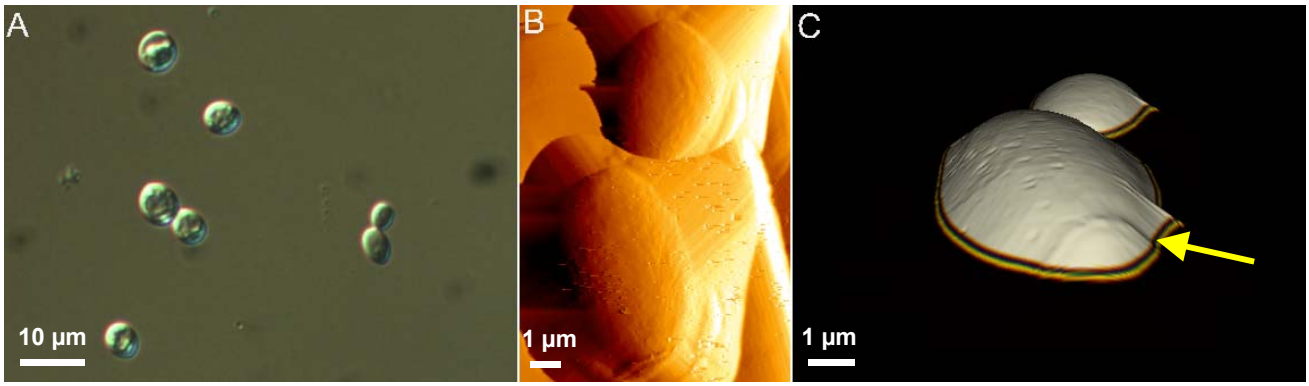

Fig. 2 Imaging of S. cerevisiae. Yeast cells were located using DIC microscopy (A) and then imaged in contact mode in fluid with the AFM (B). In (C) a 3D image generated from the height channel is displayed, highlighting the bud scar on the mother cell (yellow arrow.)

The JPK Nanowizard® BioAFM is perfectly suited to such studies. The Nanowizard® is designed to work simultaneously with light microscopy, and is installed on an inverted light microscope, allowing multiple channels of information to be collected and reducing experimental time by allowing the user to identify the location of cells of interest optically, before scanning a particular region with AFM. The specially designed sample holder, the JPK BioCell™, facilitates experiments at temperatures between 15-60°C on thin glass coverslips, such that the quality of optical images in not reduced. In addition, the JPK Nanowizard® exhibits superior stability, allowing high resolution imaging of cell components, such as bacterial surface layers (Figure 1) as well as physiological imaging of whole cells, from prokaryotes to eukaryotes.

Yeast

The yeast S. cerevisae, known also as budding yeast, is not only of use in industrial processes from bread making to the brewing of beer, it is also a type organism in the study of eukaryotic cells. As S. cerevisiae is capable of haploid or diploid growth and is a single cell organism with a doubling time of a couple of hours, it has proven well suited to the study of the basic functioning of eukaryotic cells.

The yeast S. cerevisiae is surrounded by a cell wall composed of proteins, polysaccharides and small amounts of chitin. Electron microscopy has shown that this cell wall is a layered structure ranging up to 300 nm thick. The inner layer lends mechanical strength and is composed of ß1,2-glycan and chitin. The outer layer is involved in recognition events between cells, and is mostly composed of heavily glycosylated mannoproteins. The presence of the carbohydrate side-chains on these mannoproteins make the cell wall hydrophilic and result in multiple negative charges at physiological pH. When imaged with AFM, the surface of the cell appears very smooth, and is easily deformed, necessitating careful scanning at minimal force (Figure 2). The only apparent surface feature is the bud scar at the opposite end of the mother cell to the newly forming daughter cell. The surface appears smooth as the sugars obscure the membrane.

One of the unique features of the AFM stems from the mechanical nature of the microscope itself. The flexible cantilever can be calibrated and subsequently used to calculate interaction forces (for more information, please refer to our technical report, A practical guide to AFM force spectroscopy and data analysis, tech_1204). This can then be used to determine both the force of interaction between a sample and the cantilever, and the length to which surface elements will stretch before the link to the cantilever is ruptured.

Here, we have brought the cantilever into contact with a number of points on the surface of both the mother and the daughter cell. At least 10 force-distance curves were obtained at multiple points for each cell.

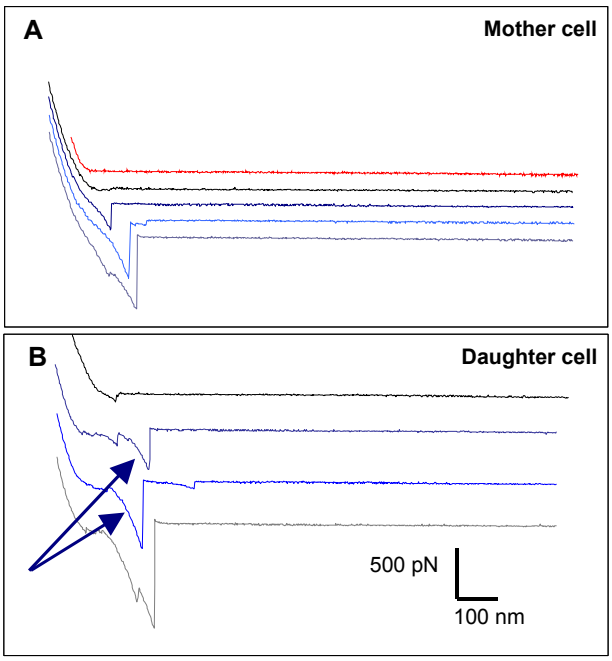

Fig. 3 Force-distance curves of the interaction between the cantilever and the surface of the daughter (A) or mother cell (B). In red is the extend curve, all others are retract curves. The maximal unbinding force (F) and separation distance (D) can be calculated from this data. The blue arrow indicates the region of the curve that is indicative of elastic stretching of the molecules.

From the force-distance curves, various data can be extracted. In Figure 3, only one of the extend curves (as the cantilever approaches the surface and deforms) has been plotted in red. The other curves all correspond to the retrace, or retraction of the cantilever away from the surface. During this retraction phase, if a surface element has bound to the cantilever, the cantilever will deflect downwards as the piezo moves the chip holding the cantilever away from the surface. As the cantilever deflects downwards the force applied to the surface element attached to the cantilever will increase. At the force at which the bond between the biomolecule and the cantilever is broken, the cantilever will snap back to its non-deflected position.

The shape of the retract section of the force-distance curves can also indicate something about the material properties of the attached biomolecule. In this case the shape of the curve shows that the surface elements attached to the cantilever deform elastically, before the interaction with the cantilever is broken. Additionally, from this retrace curve one can determine the force required to break the bond and the distance of separation from the surface at which this bond disruption occurs.

There is variability between the force-distance curves obtained on the same cell, due to the fact that not every interaction between the cantilever and the cell surface will result in the attachment of a biomolecule to the cantilever, the cantilever will not always attach to the end of a molecule and the surface composition is inherently heterogeneous. It is therefore important to acquire a sufficient number of force-distance curves so that the data can effectively be subjected to statistical analysis. Here, over 100 force curves were measured on each cell, and the maximal unbinding force, F, and separation distance at rupture, D, were calculated and are presented in Figure 4 as a histogram. The values F and D were only calculated when an interaction between a surface molecule and the cantilever was detected.

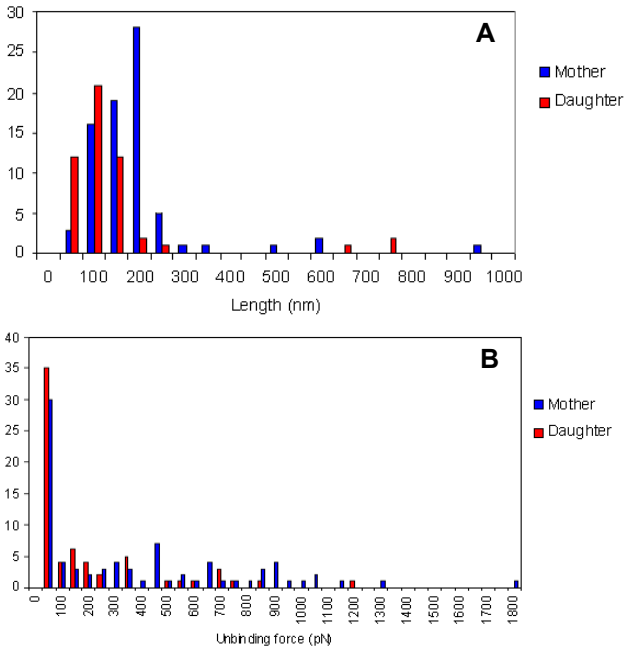

Fig. 4 Histograms of extension distance D (A) and maximal unbinding force F (B) for the mother and daughter cells.

In the case of the distance to rupture, the histogram of values shows that for both cells the data are normally distributed up to 400 nm (Fig 4A), and then for both cells there are some larger outliers. In order to compare the two data sets the outliers above 400 nm were disregarded. Within these constraints, for the mother cell D = 139 ± 56 nm, and for the daughter cell D = 86 ± 43 nm. These values were determined to be significantly different, using a two-tailed student T-test .

The data for the maximal unbinding force show that, on average, the unbinding force for the mother cell is higher than that of the daughter cell (mother, F = 352 pN: daughter, F = 167 pN). However, in this case, there is a much broader distribution of unbinding forces and in both cases, there were a number of force-distance curves where there was no deflection of the cantilever, i.e. no binding of surface molecules to the cantilever (Figure 4B). These data suggest a difference in the structure and composition of the cell wall between the mother and the daughter cell.

Bacteria

As AFM is a surface imaging technique, it has been used to characterise surface structures at high resolution. Some bacteria exhibit an S-layer, or surface layer, consisting of a regularly packed lattice of protein. The packing lends a structural stability to the sample, so isolated, crystalline S-layers can be imaged at high resolution, showing individual protein sub-units. The hexagonally packed intermediate layer from the archaebacteria Deinococcus radiodurans (Figure 1) is a well known example. In AFM images of this HPI layer, one can see the individual subunits of each pore, and that some of these pores are in an open conformation, while others are closed.

While most archaebacteria exhibit S-layers, laboratory strains of eubacteria generally do not. The most commonly used laboratory bacteria is Eschericia coli, a gram negative bacteria. Gram negative bacteria have a plasma membrane, surrounded by a periplasmic space in which there is a rigid but highly porous cell wall of peptidoglycan. This is then surrounded by an outer membrane, from which lipopolysaccarides of varying length extend.

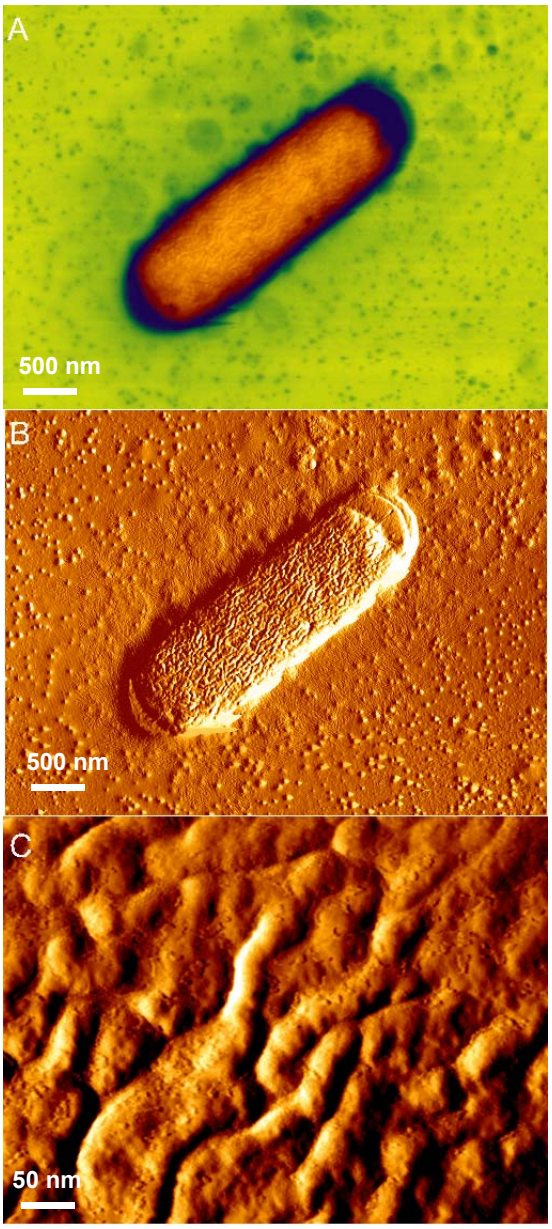

Fig. 5 Intermittent contact mode images of DH5a cells. Overview height (A) and error signal (B) images, and a higher magnification error signal image (C) of the surface of the bacterium.

Here, we have imaged two strains of E. coli, DH5a and OP50. The images of DH5a show the classic, rod-shape of many gram negative bacteria. The cells were scanned in air (Figure 5) and in buffer (Figure 6). When imaged in air, the surface of the bacteria appears highly patterned. In addition, a halo around the bacterium is apparent. These

structures likely correspond to pili, which are found at the surface of E. coli. In contrast, when imaged in fluid (Figure 6) the surface of the bacterium appears much smoother. In this case this is due to the fact that the surface structures would be easily displaced by the movement of the tip during scanning, as they are not fixed in place.

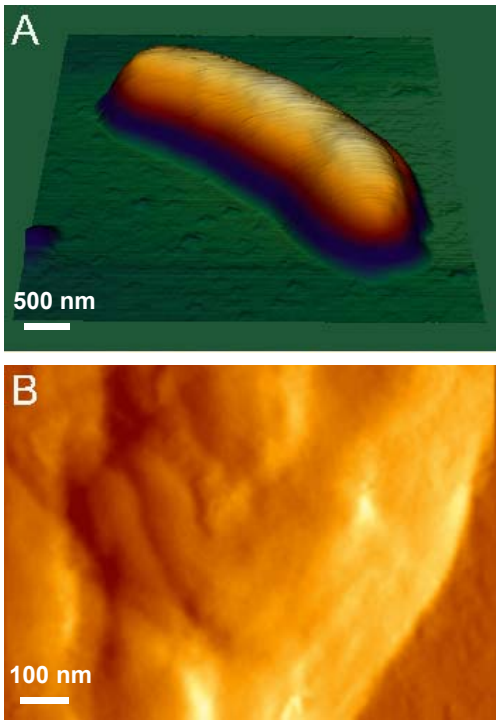

Fig. 6 Intermittent contact mode images of DH5a in fluid. A 3D image generated from topographic data (A) and a higher magnification error signal image (B) are displayed

The OP50 strain, while also E. coli, appears quite different. OP50 was originally isolated as a strain that could be used to feed Caenorhabditis elegans. It is a uracil requiring strain that is more fragile and smaller than other E. coli strains. When imaged in air (Figure 7) these bacteria do not exhibit the same structured surface as seen for the DH5a. In addition, the cells are more fragile and must be carefully imaged to avoid removing them from the surface. In fluid, the surface is also less structured than that of DH5a, and regions of the cell surface are displaced in the scan direction, likely corresponding to the displacement of the sugars and other flexible structures at the surface of the cell.

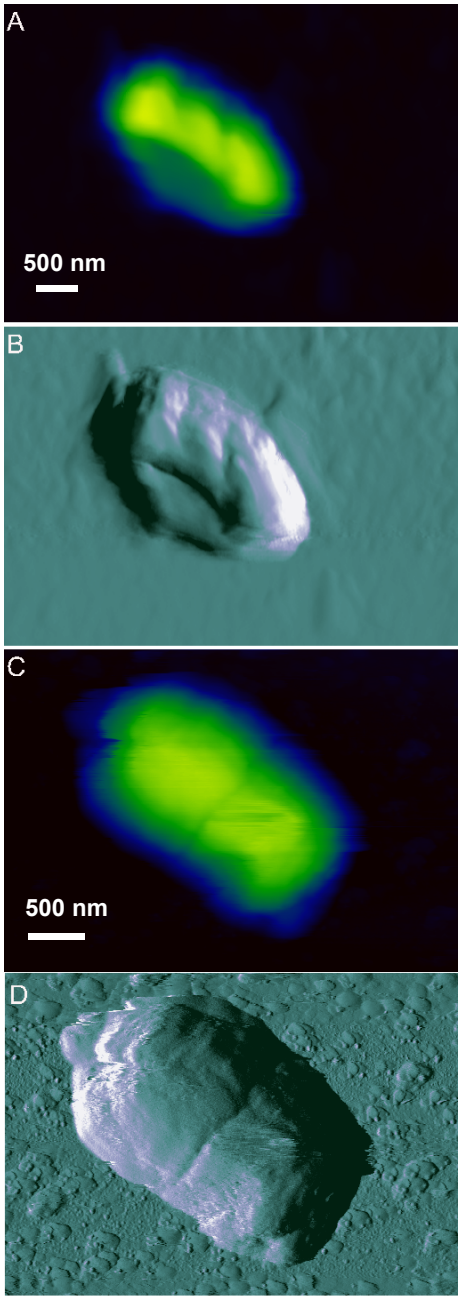

Fig. 7 Images of OP50 bacteria imaged in air (A-topography, B-error signal) and fluid (C- topography, D- error signal).

The cantilever can also be used to probe interactions with the sugars at the surface of the bacteria (as shown for S. cerevisiae above). However, here we have attached the bacteria to the cantilever (using poly-L-lysine) and measured the interaction between the bacteria and the

mica surface (Figure 8). Such a technique is unique in that it allows the quantification of bacterial-surface interactions, critical for studies of biofouling in industrial processes. The use of the JPK Biocell™ as a sample holder allows the in situ addition of compounds to block these interactions.

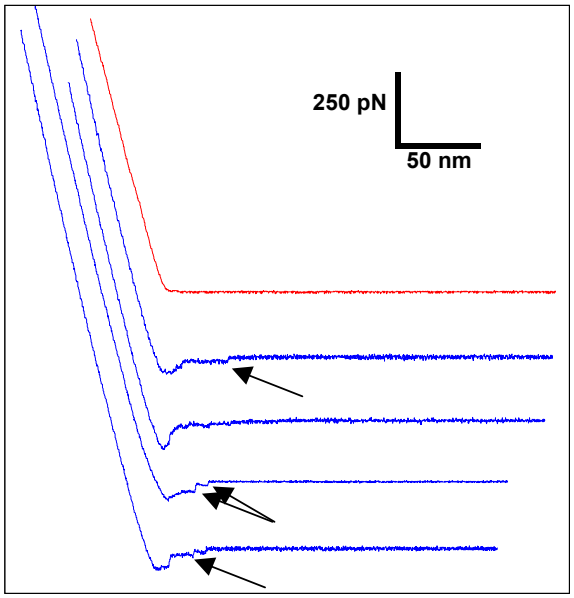

Fig. 8 Representative force-distance curvers of the interaction between cantilever-bound DH5a and a mica surface, in buffer. An extend curve is presented in red, all blue curves are retraction curves. Increasing the applied force did not increase the maximal unbinding force. Arrows indicate individual unbinding events.

Representative force-distance curves of DH5α-mica interactions are presented in Figure 8. In comparison with the interaction of the cantilever with the S. cerevisiae surface, there is no elastic deformation of the sample. A number of discrete unbinding events can be seen, likely corresponding to the unbinding of individual surface elements. Again, from the force distance curves one can quantify the maximum force required to separate the bacteria from the surface, however one can also start to investigate individual unbinding events.

Viruses

Viruses are obligate intracellular parasites composed of an outer protein coat surrounding genetic material that consists of either DNA or RNA. This genetic material does not contain all the information required for replication, instead the virus needs to subvert the cellular machinery of the host cell to propagate. Viruses are extremely small, around 20 nm to 400 nm. This means that the characterisation of viral structure requires high resolution imaging techniques, such as atomic force microscopy. Here we have imaged tobacco mosaic virus (TMV), the first virus imaged using electron microscopy.

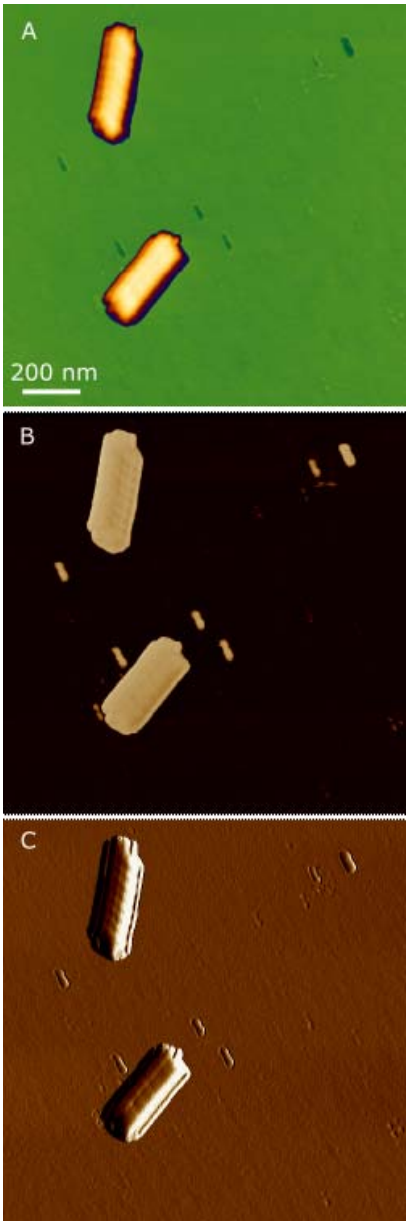

Fig. 9 Intermittent contact mode images of TMV particles. Topography (A), phase (B) and error signal images (C) of the same sample region are presented.

The TMV particles were adsorbed to mica and imaged using intermittent contact mode. These virus particles are known as helical capsids, where the coat protein stacks in a helical pattern around the genetic material. This helical stacking can be seen in the height, phase and error signal channels (Figure 9). One significant advantage of using a BioAFM, such as the JPK Nanowizard®, to image biological samples, is that the imaging can be conducted in fluid. As such, virus particles can be imaged on the surface of their target cells, in fluid. Here, we have imaged influenza virus attached to the surface of red blood cells, in fluid, using intermittent contact mode. The virus particles are clearly imaged at the surface of the cells.

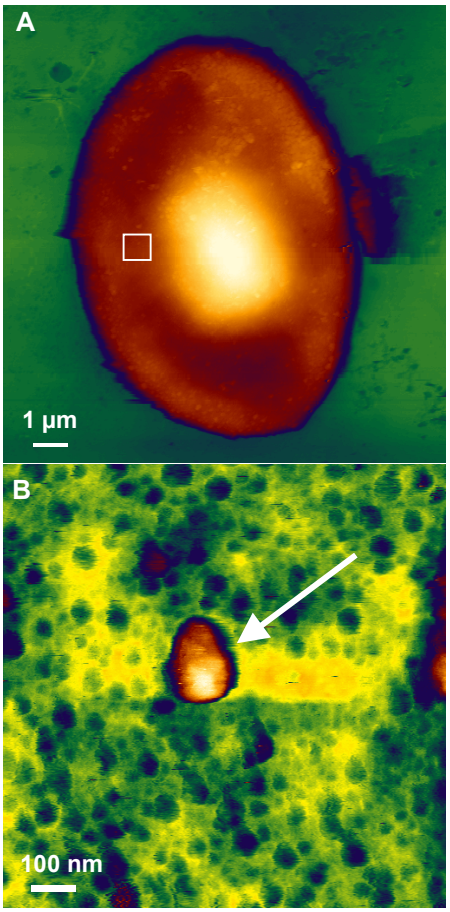

Fig. 10 Influenza virus particles associated with the surface of an erythrocyte. The overview image (A) and higher magnification image (B) of the red blood cell surface show influenza virus particles (white arrow)

Conclusions

The Nanowizard® bioAFM is perfectly suited for the study of microorganisms. The JPK Biocell provides physiological conditions without sacrificing AFM stability or optical quality. The stability of the microscope enables imaging of individual protein subunits, and full integration into an inverted light microscope enables a combination of microscopy techniques to be conducted simultaneously. Not only does this platform allow high resolution images of microbial samples, it can be used to quantify interaction forces between organisms and a surface or between the cantilever and surface-associated molecules.

Acknowledgements

Many thanks to Dr. Jeffrey Stear, Max Planck Institute for Molecular Cell Biology and Genetics, for the E. coli and S. cerevisiae samples. TMV was kindly provided by Dr. Michael Laue from the Robert Koch Institute. The HPI images were kindly provided by Dr. Patrick Frederix, University of Basel.

References:

[1] Benoit M., Gaub H.E. "Measuring cell adhesion forces with the atomic force microscope at the molecular level". Cells Tissues Organs. 172:174-89. (2002)

[2] Zhang X., Chen A., De Leon D., Li H., Noiri E., Moy V.T., Goligorsky M.S. "Atomic force microscopy measurement of leukocyte-endothelial interaction". Am. J. Physiol. Heart Circ. Physiol. 286:H359-67. (2004)

[3] Puech P.H., Taubenberger A., Ulrich F., Krieg M., Muller D.J., Heisenberg C.P. "Measuring cell adhesion forces of primary gastrulating cells from zebrafish using atomic force microscopy". J. Cell Science, 118:4199-206. (2005)

[4] Ulrich F., Krieg M., Schötz E.M., Link V., Castanon I., Schnabel V., Taubenberger A., Mueller D., Puech P.H., Heisenberg C.P. "Wnt11 functions in gastrulation by controlling cell cohesion through Rab5c and E-Cadherin". Developmental Cell, 9:555-64. (2005)

[5] Haass N.K., Smalley K.S., Li L., Herlyn M. "Adhesion, migration and communication in melanocytes and melanoma". Pigment Cell Res. 18:150-9. (2005)

[6] Poole K., Muller D. "Flexible, actin-based ridges colocalise with the beta1 integrin on the surface of melanoma cells". Br. J. Cancer. 92:1499-505. (2005)

[7] Puech P.H., Poole K., Knebel D., Mueller D.J. "A new technical approach to quantify cell-cell adhesion forces by AFM". Ultramicroscopy. 106: 637–644 (2006).